Japan-US Workshop on
Fusion Power Plants and Related Advanced Technologies
February 23 - 24, 2010 at UCSD

Recent activities on FFHR designs towards DEMO

Akio Sagara

with FFHR design group :
S. Imagawa[1], O. Mitarai[2], T. Goto[1], T. Tanaka[1], T. Watanabe[1], N. Yanagi[1], Y. Kozaki[1],
H. Tamura[1], Y. Suzuki[1], K. Takahata[1], S. Masuzaki[1], M. Shoji[1], M. Kobayashi[1],
K. Nishimura[1], T. Muroga[1], T. Nagasaka[1], M. Kondo[1],
H. Igami[1], H. Chikaraishi[1], S. Yamada[1], T. Mito[1],
S. Fukada[3], H. Hashizume[4]

[1]National Institute for Fusion Science, Toki, Gifu, Japan
[2]Tokai University, Kumamoto, Japan
[3]Kyushu University, Fukuoka, Japan
[4]Tohoku University, Sendai, Japan

FFHR2m2
3GWth
5 Tesla
30,000 ton

Presentation outline

1. Reactor size optimization
2. Divertor system
3. Helical SC magnet system
4. Blanket system
5. Plan towards Helical DEMO

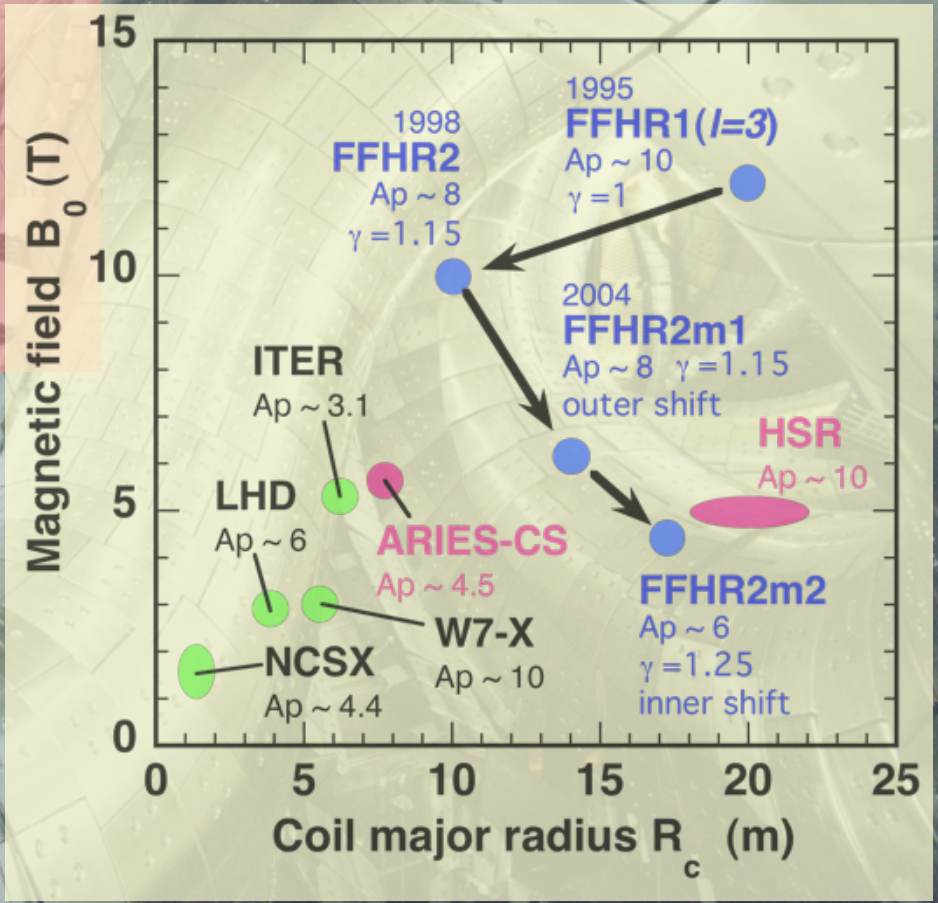

Target and Achievements in LHD

Achievements [Final target]

Ion Temperature

Central T_i 5.2 keV [10 keV]
Density $1.2\times10^{19}m^{-3}$ [$2\times10^{19}m^{-3}$]

Central T_i 13.5 keV
Density $3\times10^{18}m^{-3}$ (Ar gas)

Electron Temperature

Central T_e 10 keV [10 keV]
Density $5\times10^{18}m^{-3}$ [$2 \times 10^{19}m^{-3}$]

> 10 keV : reactor condition

Volume Averaged β

5.0 % (magnetic field of 0.425T)
[≥ 5 % (1-2 T)]

> 5% : reactor condition

Steady State Operation

31min.45sec. (680 kW) 1.3GJ [1 hour (3,000 kW)]
54min.28sec. (490 kW) 1.6GJ

Largest input energy

High Density
$1\times10^{21}m^{-3}$

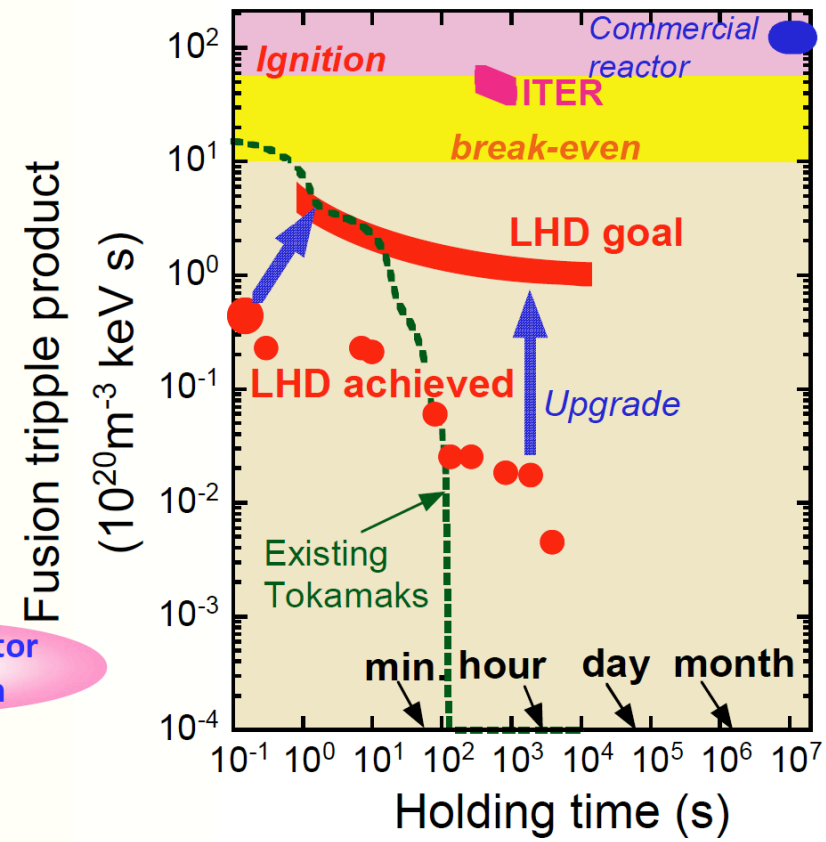

Highlighted progress in
Steady State, High β, and
High Density
by discovery of
Internal Diffusion Barrier (IDB)

Accumulation of physical data
Systematic investigations become possible
➔ increase of heating power, deuterium experiment, etc.

Because of current-free plasma, Stellarator/Heliotron have attractive advantages

non-axisymmetric configurations originate challenging subjects on physics and engineering

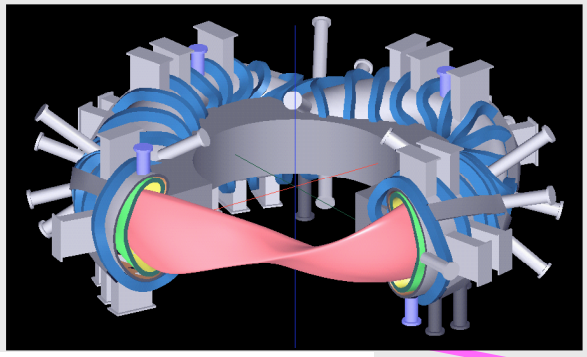

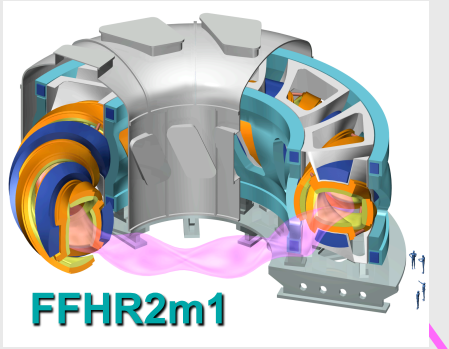

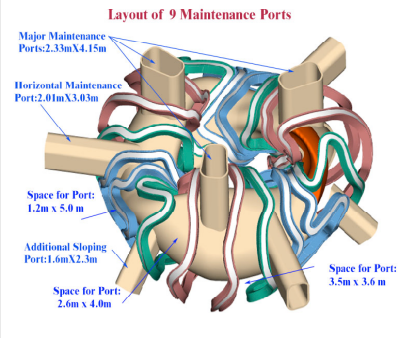

HSR based on W7-AS & W7- X

based on LHD

ARIES-CS based on NCSX

	11.7	T-1	UWTOR-M	MSR	CT6	HSR	FFHR 2m1	MHR-S	SPPS	ARIES-CS
Main field coils	2	3 (modular)	3 (modular)	2(modular)	2	50 (modular)	2	2(modular)	32(modular)	18(modular)
Toroidal field periods	15	20	6	6	6	5	10	10	4	3
Major radius (m)	21	29.2	24.1	20.2	6.57	20	14	16.5	13.95	7.75
Average plasma radius (m)	1.8	2.3	1.35	1.84	1.74	1.6	1.73	2.36	1.6	1.7
Plasam sspect ration	11.7	12.7	14	11	3.8		8.1			
Toroidal field on axis (T)	4	5	5.5	6.4	6	5	6.2	5	4.95	5.7
Maximum field (T)	9	8.7	9.5	13	16	10.6	13.3	14.9	14.5	15.1
Magnet current density (A/mm^2)	22	30	12.5	19	55	25	26.6	30		100
Stored magnetic energy (GJ)		460	190	200		74	133	221	80	
Plasma volume (m^3)	1343	3240	1408	1340	394	1000	827		735	444
Average beta (%)	6%	3.54%	5%	4%	4.70%	4-5%	3%	5%	5%	6%
Fusion output (GW)	3.4	4.3	5.5	4	1.8	~ 3	1.9	3.8	2.29	2.44
Alpha heating efficiency				0.88	0.58		0.9			
Plasma density $n_e(0)$ (x10^{20} /m^3)	average <1.17>	<1.3>		<1.72>	<3.18>	2.8	2.8	4	<1.46>	
Plasma temperature Ti(0) (keV)	average <10.3>	<7.33>		<8.0>	<6.84>	15	15.3	15.6	<10>	
Plasma-magnet space (m)		1.5		1.5	0.9	1.1	1.1	1.14		1.21
T-breeder	Li2O	Li	Li17Pb83		6Li17Pb83	HCPB / LiPb	Flibe		Li	LiPb
Net tritiumu breeding ratio	1.17				1.05		1.08			
Structure material	SUS		HT-9		HT-9	SS, FS	FS		V	FS
Neutron wall loading (MW/m^2)	1.3	1	1.72	1.5	2.8	1.2	1.5-1.8	1.9	1.18~2.11	2.6-5.4
COE (mill/kWh)					67	97.8	106		74.6	78
	1974 ~ 1982	1978	1981	1981	1989 ~	1992 ~	1995 ~	1996 ~	1997	2002~
	Kyoto-U	MIT	Wisconsin-U	Los Alamos Princeton	ORNL	IPP-Garching	NIFS	NIFS	ARIES	ARIES
references	5, 6	7	8	9	10	14	11, 12	13	15	16

A. Sagara :1998.6.2,5 (rev. 2010.03.11)

Design parameters

Design parameters			LHD	FFHR2	FFHR2m1	FFHR2m2	SDC
Polarity	l		2	2	2	2	
Field periods	m		10	10	10	10	
Coil pitch parameter	γ		1.25	1.15	1.15	1.20	
Coil major Radius	R_c	m	3.9	10	14.0	17.3	
Coil minor radius	a_c	m	0.98	2.3	3.22	4.16	
Plasma major radius	R_p	m	3.75	10	14.0	16.0	
Plasma radius	$\langle a_p \rangle$	m	0.61	1.24	1.73	2.35	
Plasma volume	Vp	m^3	30	303	827	1744	
Blanket space	Δ	m	0.12	0.7	1.1	1.05	
Magnetic field	B_0	T	4	10	6.18	4.84	
Max. field on coils	B_{max}	T	9.2	14.8	13.3	11.9	
Coil current density	j	MA/m^2	53	25	26.6	26	
Magnetic energy		GJ	1.64	147	133		
Fusion power	P_F	GW		1	1.9	3	
Neutron wall load	Γ_n	MW/m^2		1.5	1.5	1.5	
External heating pow	P_{ext}	MW		70	80	43	100
α heating efficiency	η_α			0.7	0.9	0.9	0.9
Density lim.improvement				1	1.5	1.5	7.5
H factor of ISS95				2.40	1.92	1.92	1.60
Effective ion charge	Z_{eff}			1.40	1.34	1.48	1.55
Electron density	$n_e(0)$	$10^{19}\ m^{-3}$		27.4	26.7	17.9	83.0
Temperature	$T_i(0)$	keV		21	15.8	18	6.33
Plasma beta	$\langle\beta\rangle$	%		1.6	3.0	4.40	3.35
Plasma conduction lo	P_L	MW			290	453	115
Diverter heat load	Γ_{div}	MW/m^2			1.6	2.3	0.6
Total capital cost	G$(2003)			4.6	5.6	7.0	
COE	mill/kWh			155	106	93	

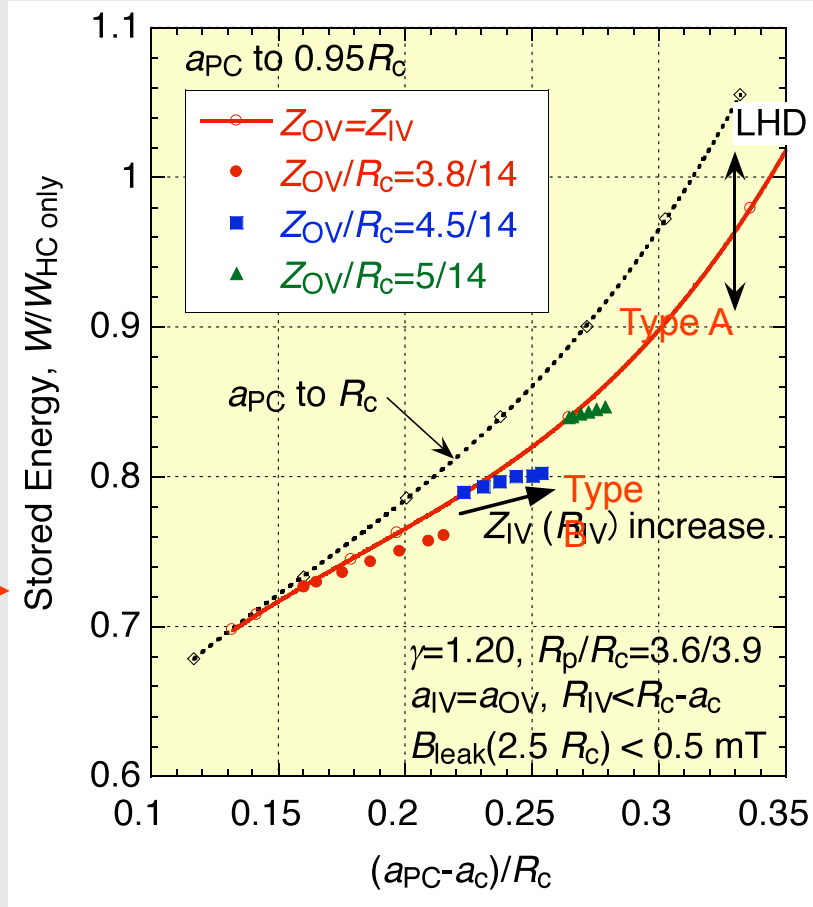

In SDC,
divertor heat load is
drastically reduced (~1/4).

Will be presented for NBI at IAEA FEC 2010 by O.Mitarai

By T. Watanabe

D-T α orbits extending to the chaotic field line region.

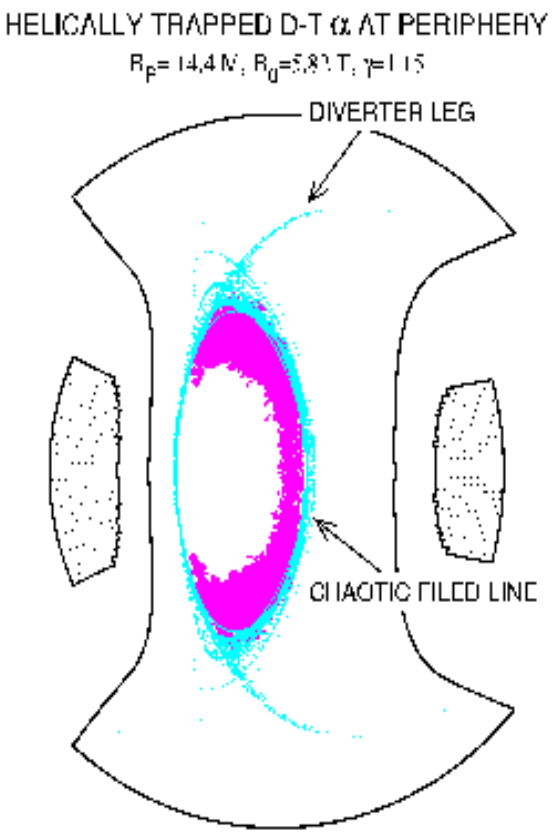

Poincare plot of helically trapped α particles (magenta dots) and the chaotic field lines (sky blue dots).

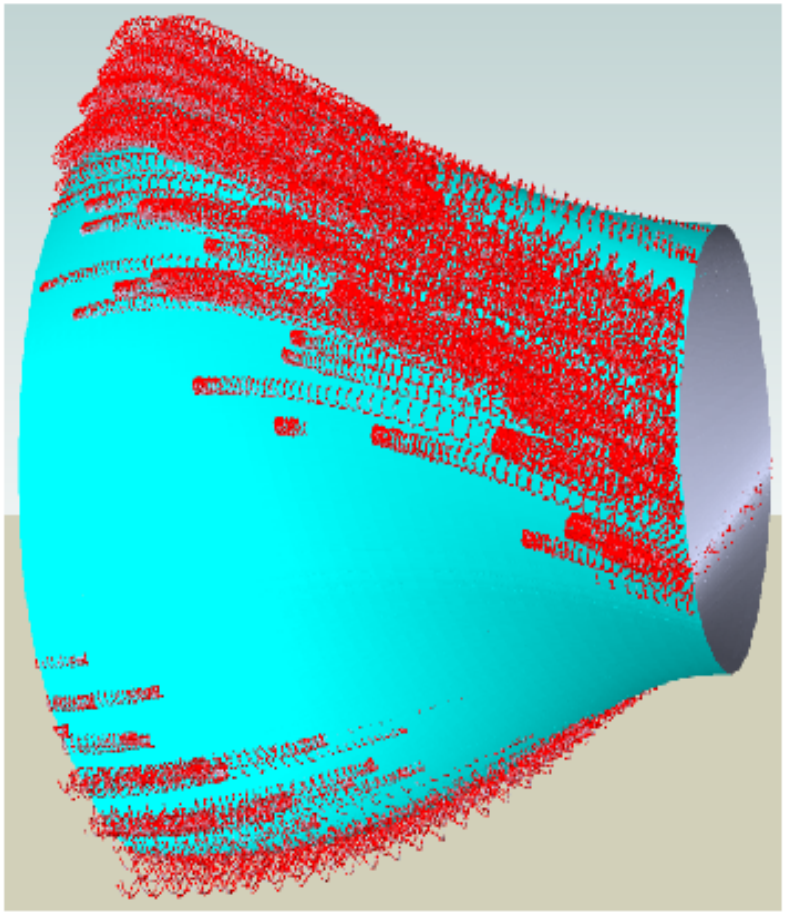

3D view of the particle orbits and the last closed flux surface(painted by sky blue).

Vacuum magnetic surfaces of FFHR-2m2

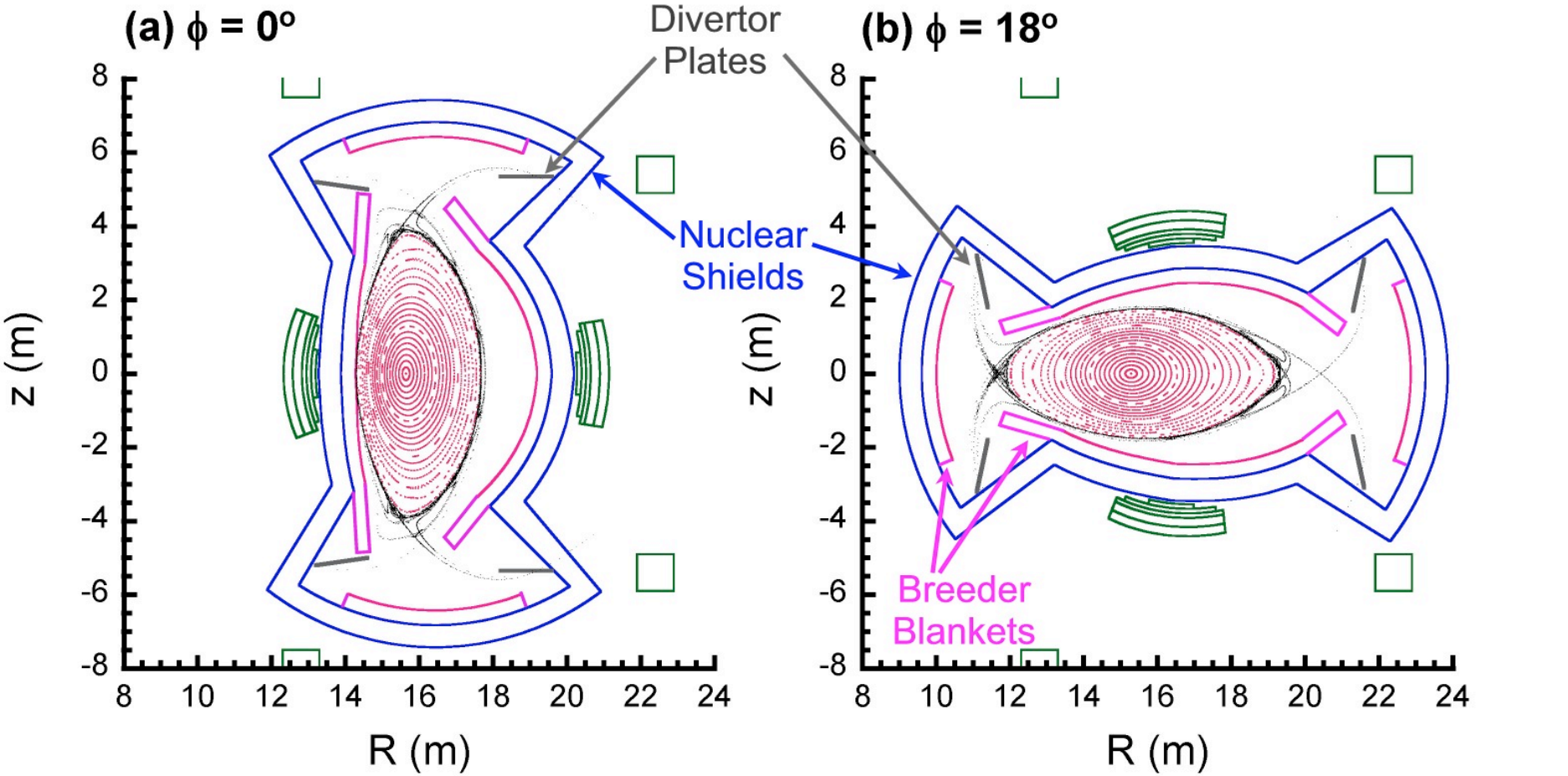

R_c = 16.74 m, R_p = 16.0 m, γ = 1.2, α = +0.1, B_p = 4.84 T, j_{HC} = 25 A/mm^2

- Latest design "FFHR-2m2 Type-D" with maximized magnetic surfaces by optimization of poloidal coil positions and currents

High-beta equilibrium for FFHR

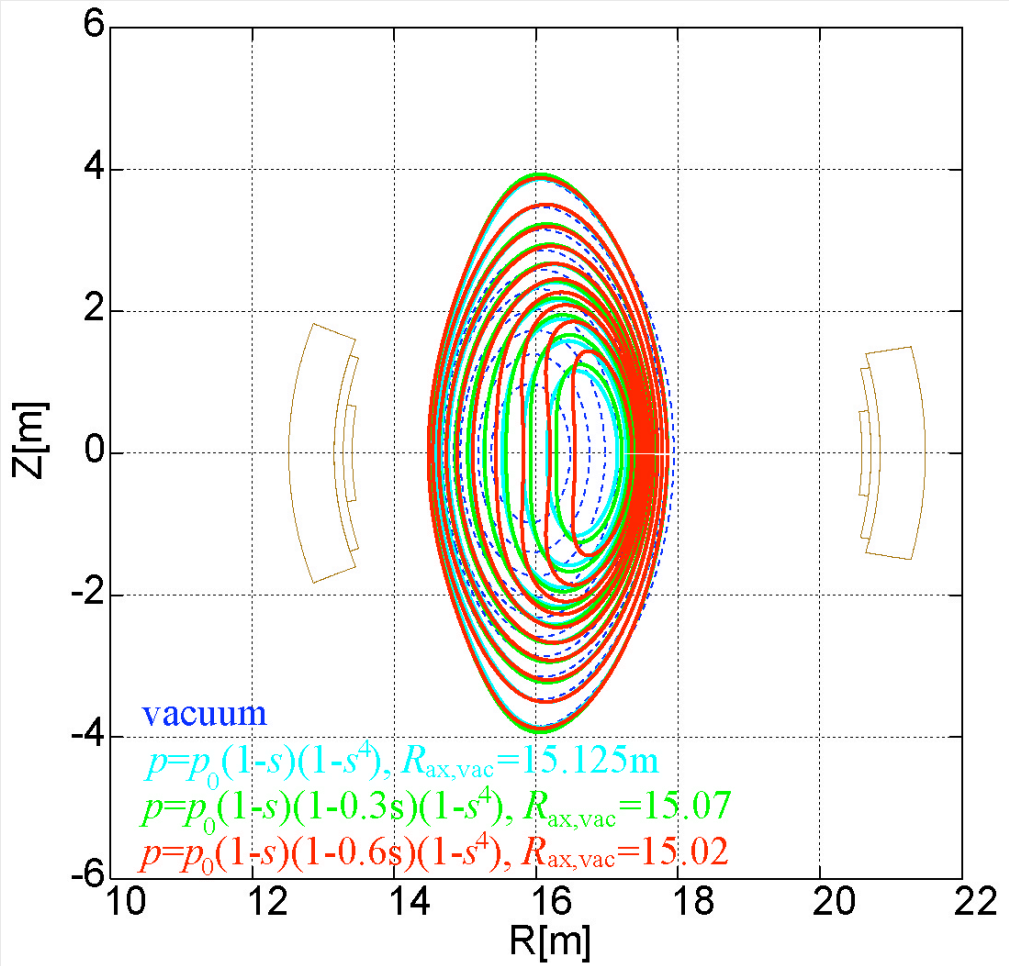

Parameters consistent with the FFHR design

- ✓ LCFS volume : 1942m^3 (1967m^3)
- ✓ Volume-averaged beta : 5.5%
- ✓ Plasma stored energy : 1329MJ (1305MJ)

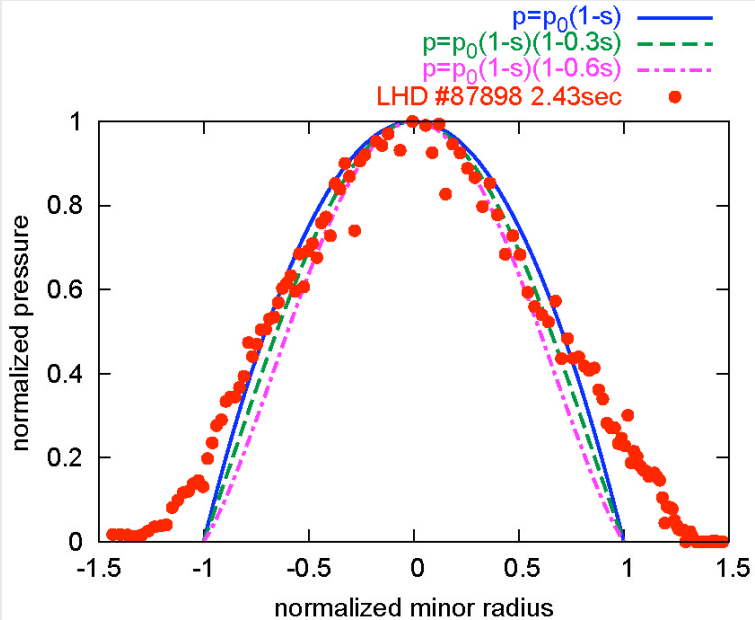

- **High-beta (<β>=5.5%) equilibrium with the volume enclosed by LCFS as large as vacuum equilibrium was confirmed by VMEC calculation.**

System design code has been developed

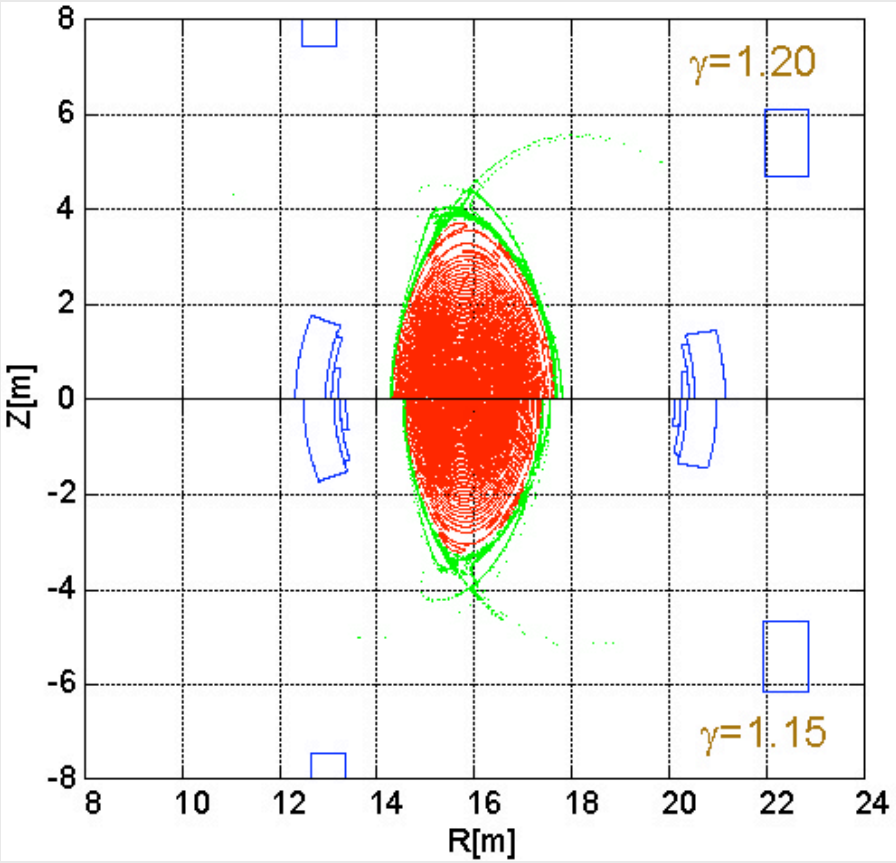

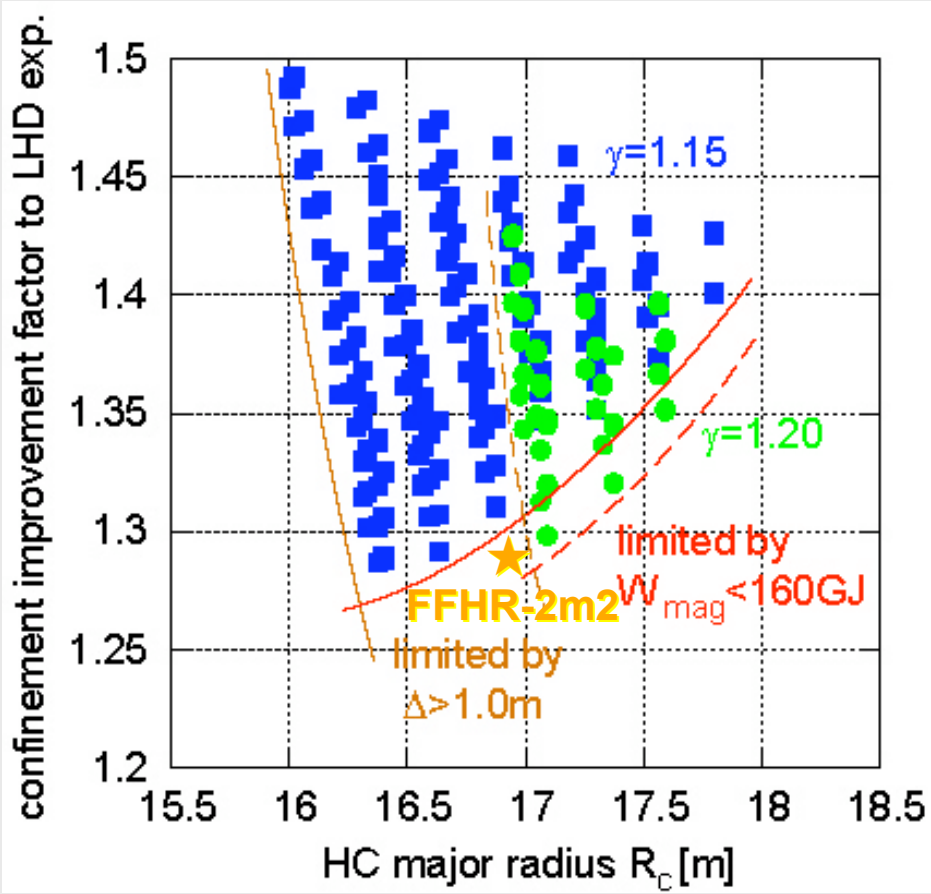

- **System design code for LHD-type heliotron reactors has been developed.**
- **Parametric scans with actual geometry of helical / poloidal coils has been advanced.** *Will be presented at IAEA FEC 2010 by T.Goto*

Optimization trial with split-type helical coils

- Larger inboard space is attained by splitting helical coils in the outboard side
- Further merits are pursued with optimization of conventional heliotrons

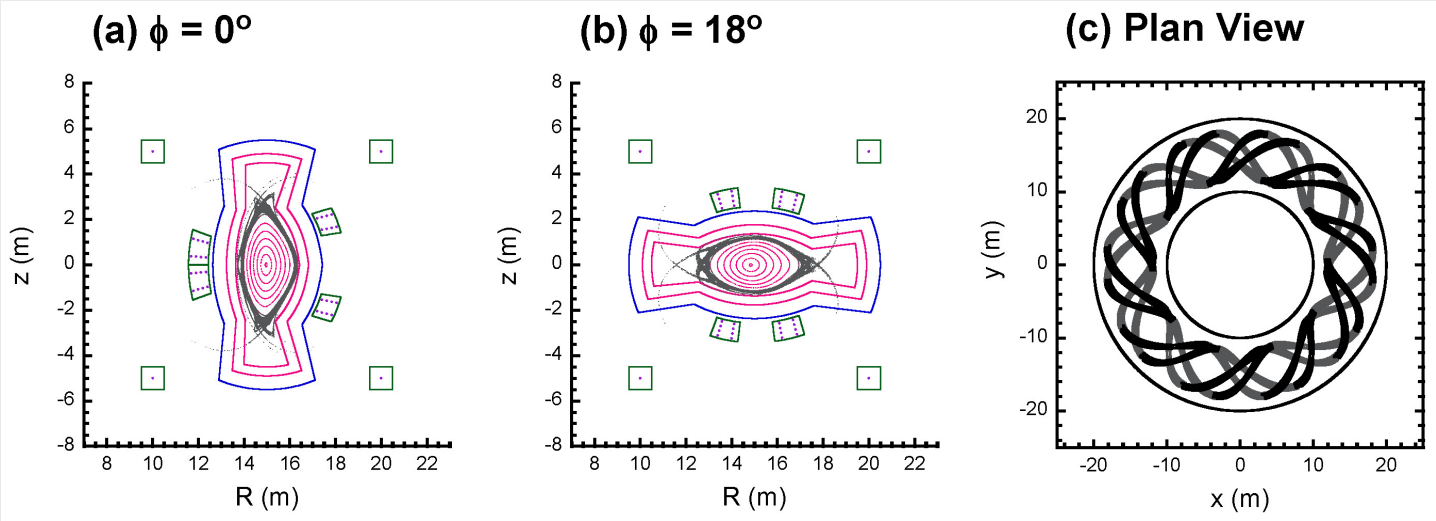

FFHR-2S Type-I

R = 15.0 m, γ = 1.0

- smaller size
- higher field

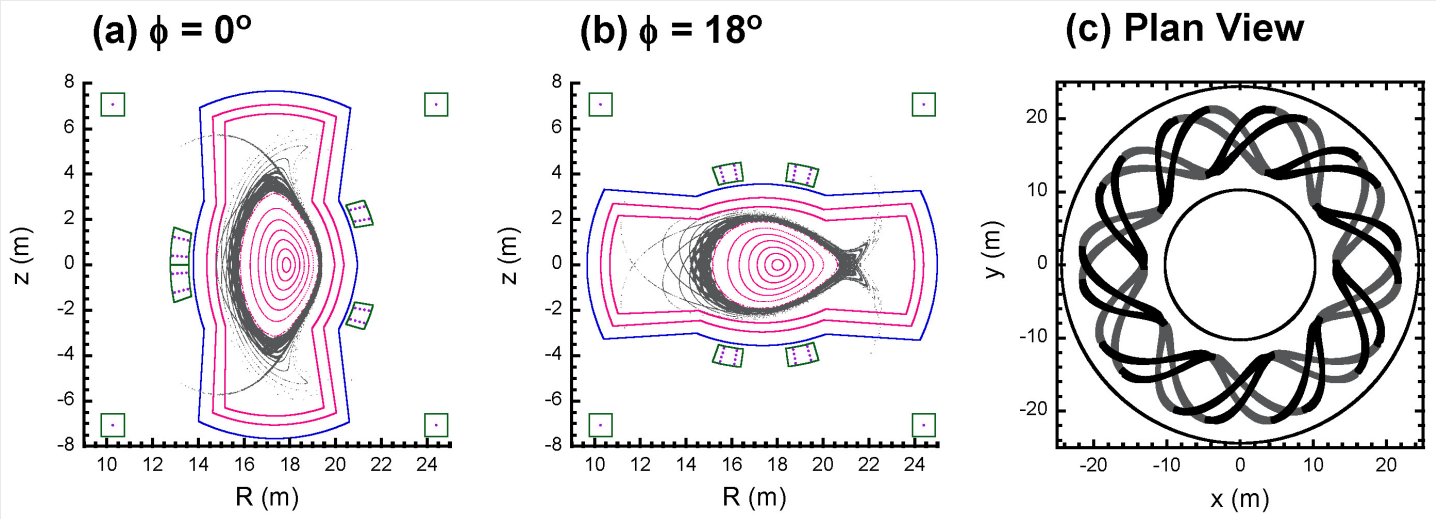

FFHR-2S Type-II

R = 17.3 m, γ = 1.2

- larger surfaces
- deeper well

Presented at ISHW17 (2009) by N. Yanagi

Advantage of Low γ - Flat type Helical Coil System

Relation between magnetic surface, diverter leg and blanket modules

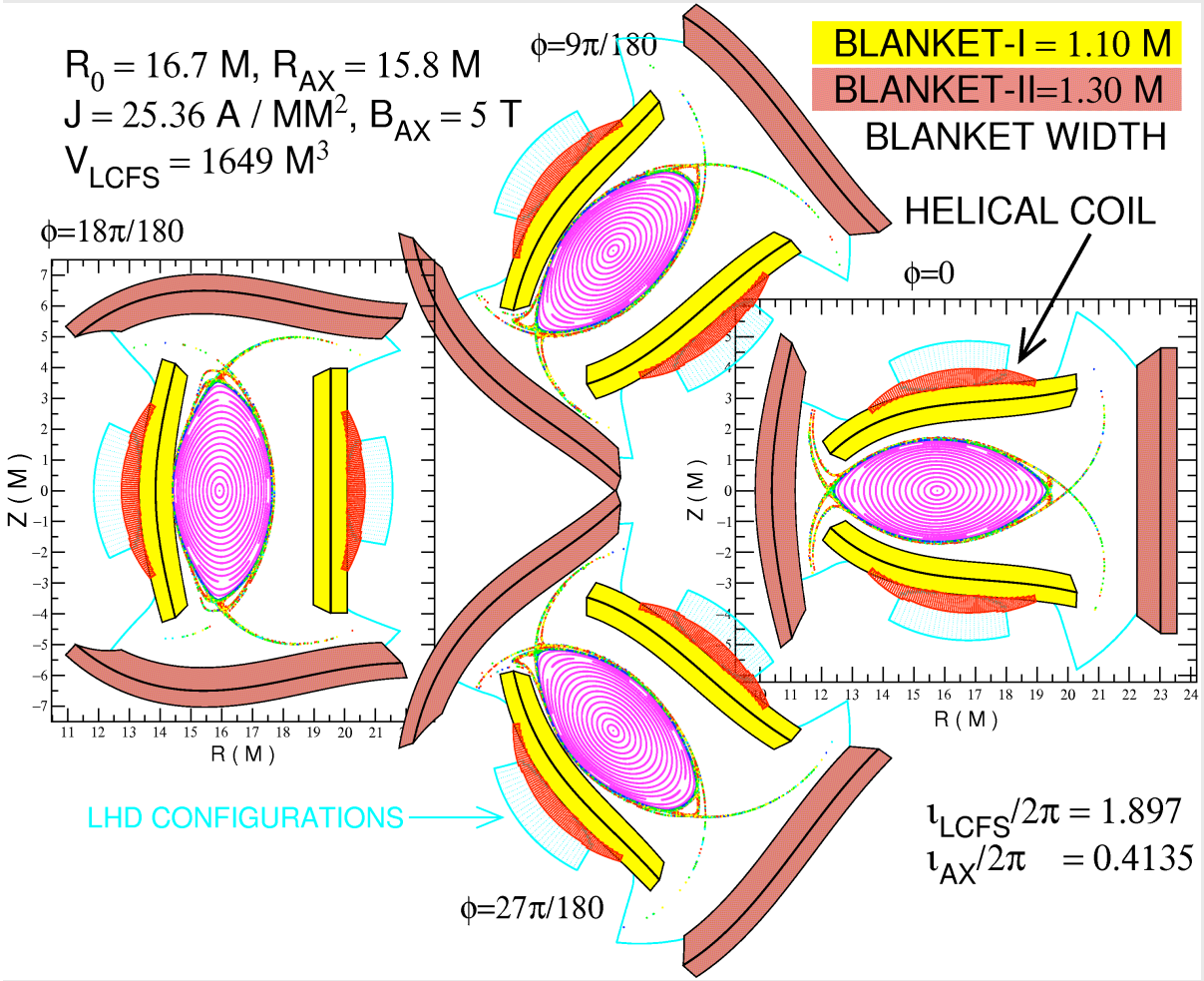

The following possibilities are shown in the left figure.

1. Installation of TBM of high coverage with enough thickness.
2. Closed diverter system.

Because the coils are flat type, the following are expected.

1. Reduction of magnetic stress on helical coils.
2. Ensuring of liquid helium path for helical coils.
3. Neutron shielding on the back of helical coils.

Favorable magnetic field configuration by low γ helical coils.

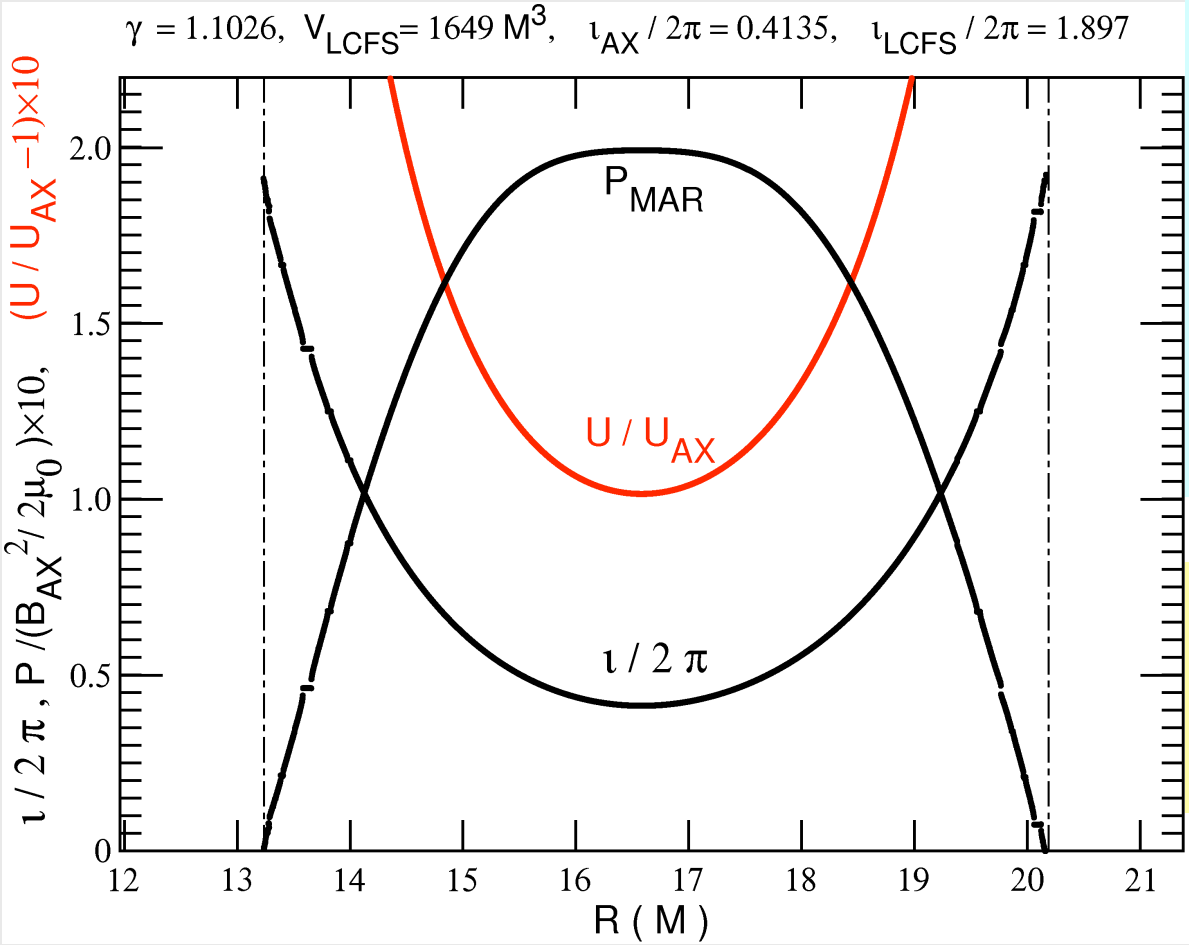

Vacuum magnetic field configuration is shown in the left figure.

1. Rotational transform iota.
2. Magnetic hill U.
3. Marginally MHD stable pressure profile Pmar.

Low γ magnetic field configuration is favorable for high beta plasma confinement*.

*T.Watanabe, A.Sagara, submitted to PFR, 2009.

Divertor sweeping with Helical Divertor Coils

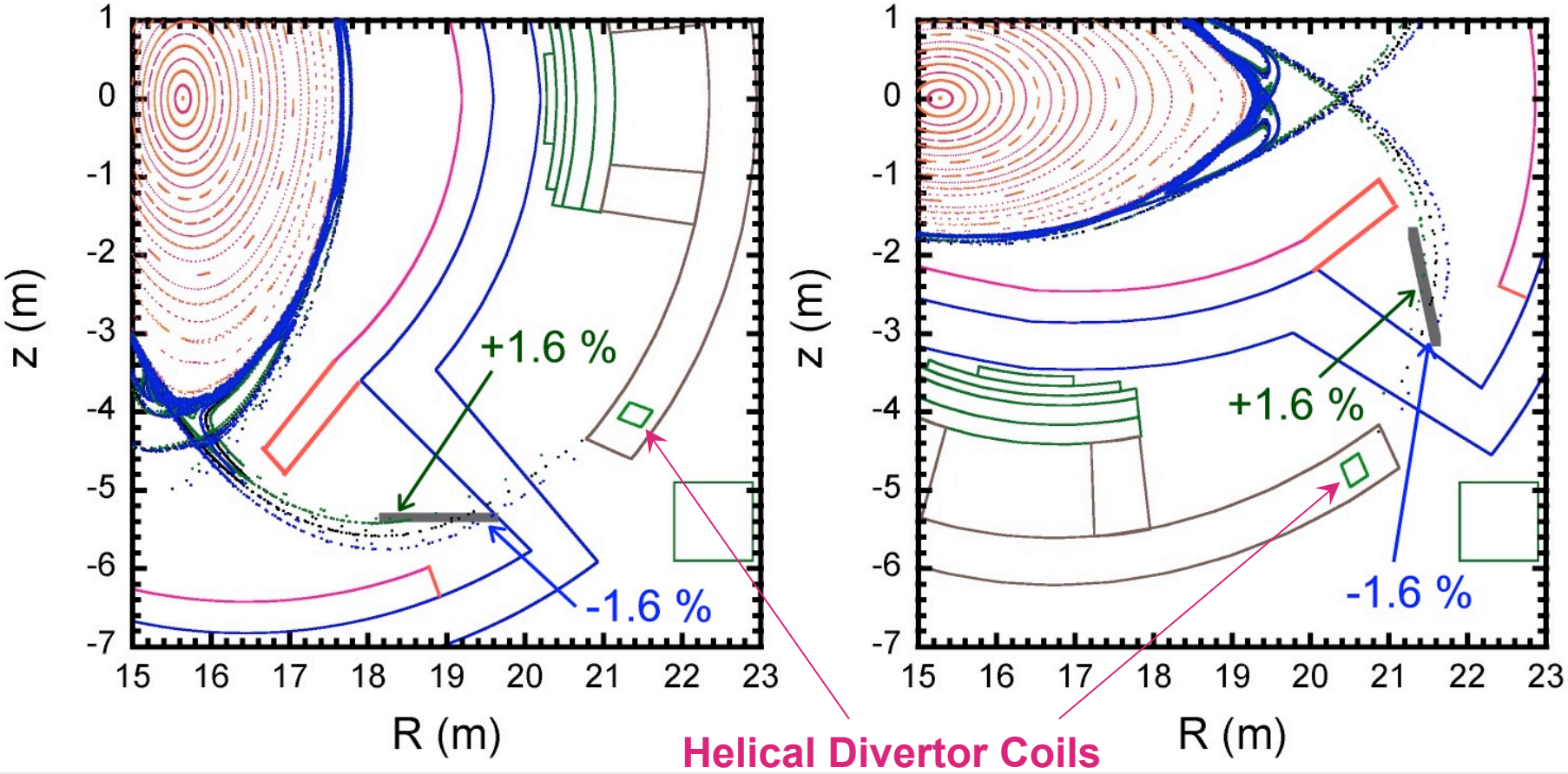

Strike points are effectively swept by AC operations of "Helical Divertor Coils" with 2-3 % of main helical coil currents and no change of magnetic surfaces

Total wetted area : ~700 m2 ➔ Divertor heat flux : <1 MW/m2 (on average)

Will be presented at IAEA FEC 2010 by N. Yanagi

High-temperature superconductors to be applied for helical divertor coils

- Total current of 750 kA (2% of main helical coil currents) = 30 kA ×25 turns
- YBCO-based HTS conductor : probable candidate (also for the main coils)
- Could be constructed in segments (jointed onsite and remountable)
- AC operations with 0.025 Hz (40 s cycle) : no problem for HTS at 30 K or higher
- R&D successfully started with 10 kA-class YBCO conductors

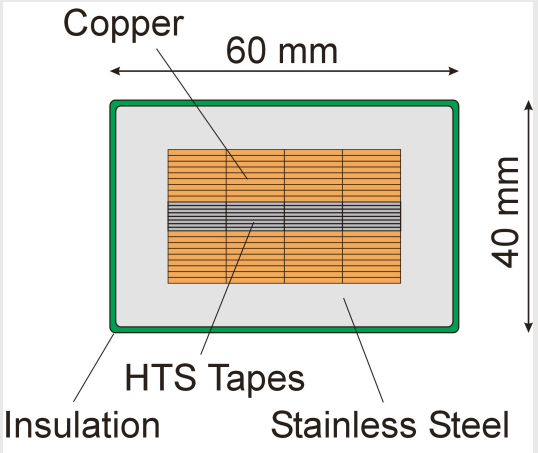

100 kA HTS conductor design

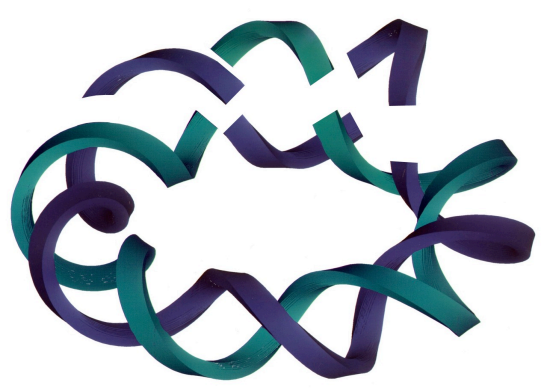

Segmented fabrication of helical coils

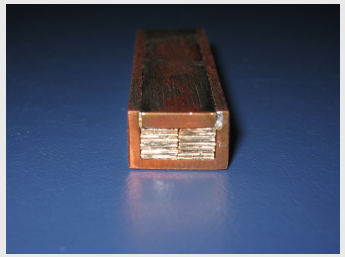

10 kA HTS conductor

Will be presented at IAEA FEC 2010 by N. Yanagi

Concept of Heliotron DEMO with Q>20

	H-Power plant	H-Demo	ITER
H-factor of τE, HH	1.2 to LHD	←	
Energy gain, Q	∞ (self ignition)	> 20	10
TBR	> 1.0	> 1.0	
Min. blanket thickness [m]	> 1.0	> 0.8	
Fusion power [GWth]	4 - 5	1.8	0.5
Major radius of plasma [m]	15-16	13.4	
Max. field [T]	11-12	11.0	11.8 (TF)
Stored magnetic energy [GJ]	120-150	~90	41 (TF)

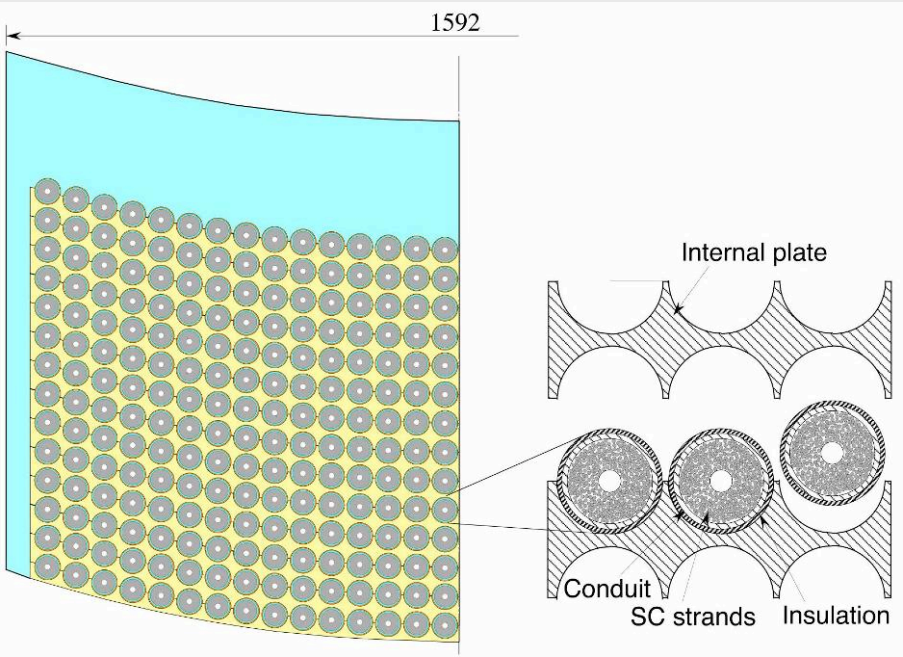

Layer winding by 5 in hand with CICC

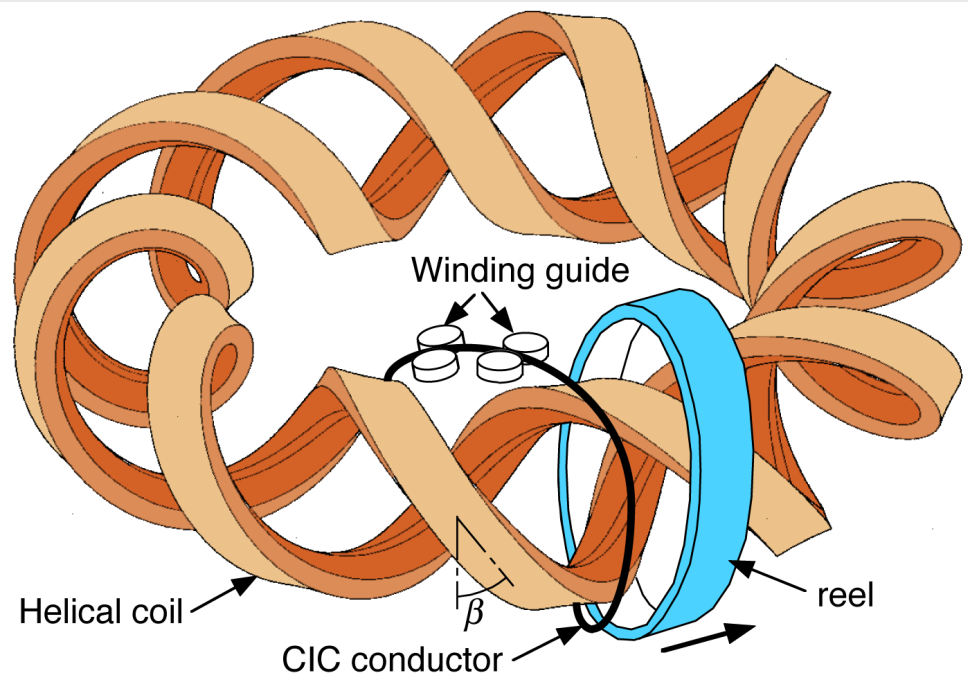

Concept of Helical Coil with CICC

React and Wind method can be applied by using Nb3Al.

<Strain by transfer of conductor to reel>

Radius of the reel : 5.71 m

Radius of the SC cable : 0.0165 m

Strain at transfer : 0.15%

(0.0165/5.71-0.0165/12=0.15%)

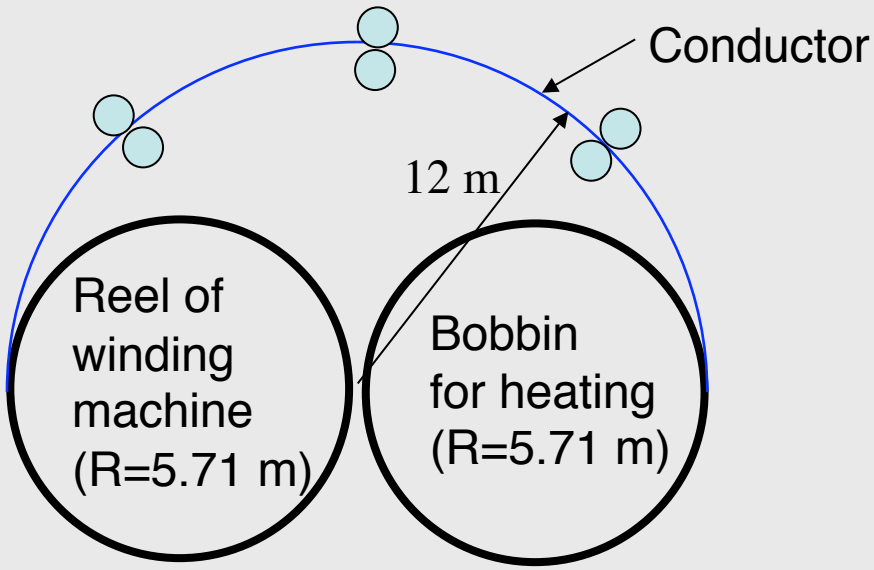

<Shear strain by winding>

$$\langle r\theta \rangle = \frac{r \cdot tan^{-1}\beta}{2\pi a_c / 4} \approx 0.3\%$$

$$r\theta < 0.6\%$$

This strain is considered to be allowable for Nb3Al strands. Helical winding with CIC conductors must be demonstrated.

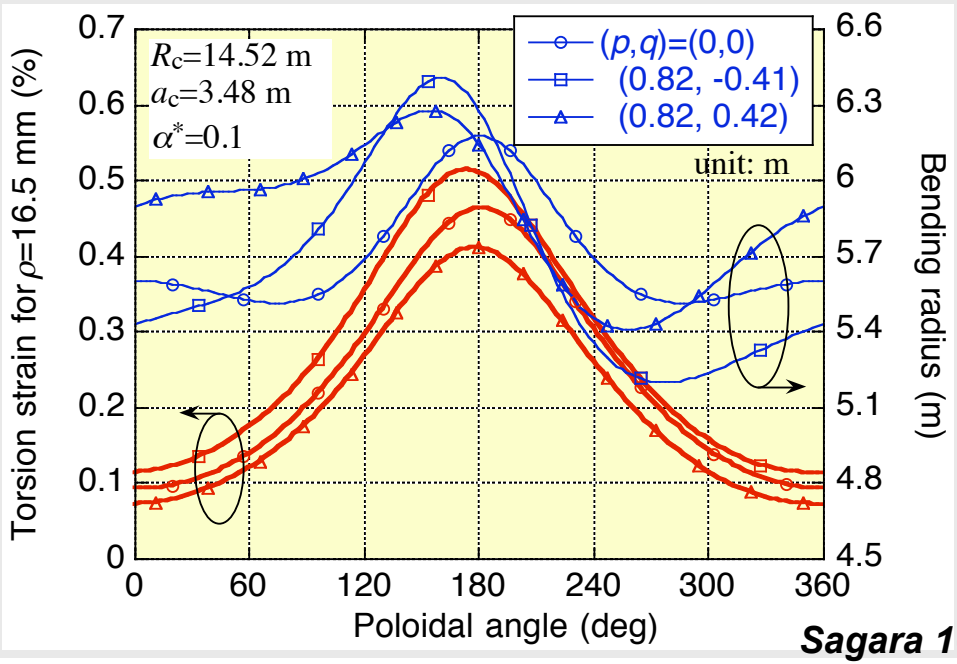

R&D of an indirect-cooled superconductor

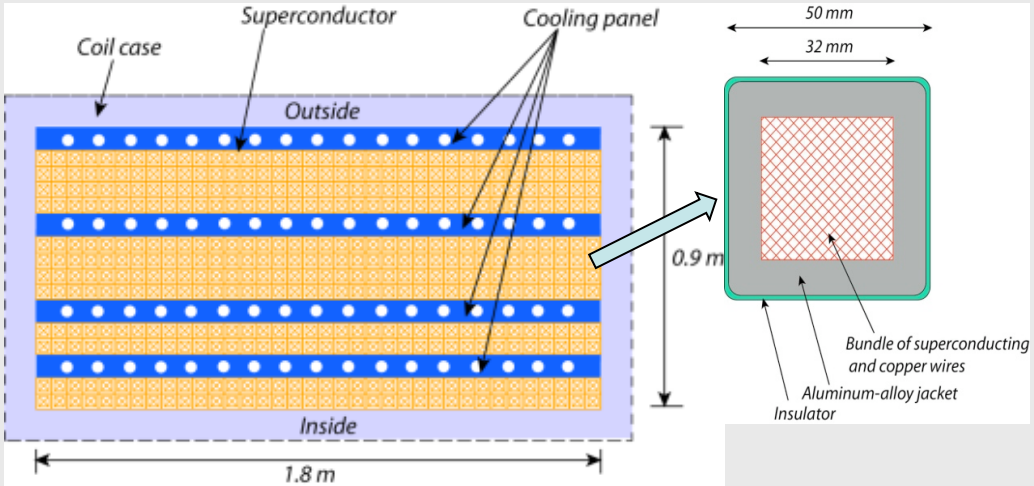

Schematic of an indirect-cooled superconducting magnet and a superconductor.

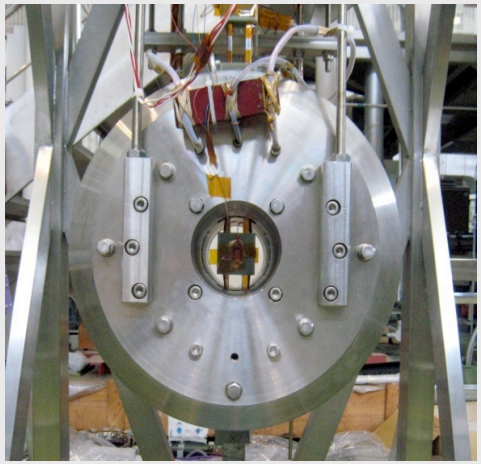

Sample set up in the 8T sprit coil.

1. The possibility of using an indirect-cooled superconducting magnet to the LHD-type fusion reactor has been investigated.
2. Nb_3Sn superconductor jacketed with an aluminum alloy has been developed, and the results of performance tests for a sub-scale superconductor showed good feasibility. **Stable manufacturing with FSW** has been achieved.

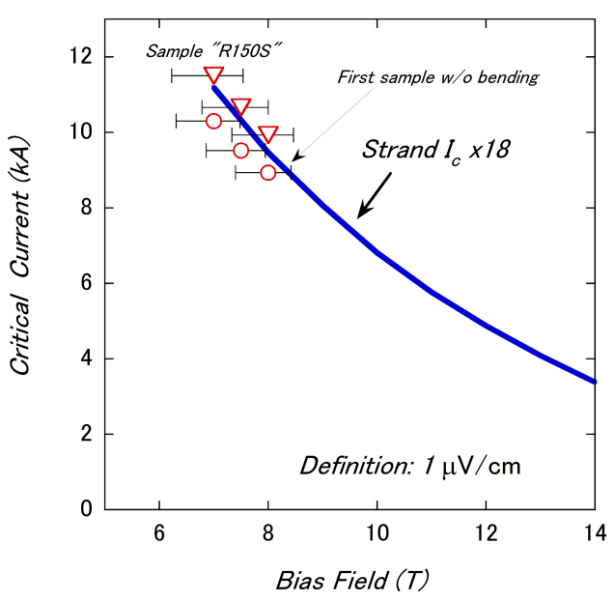

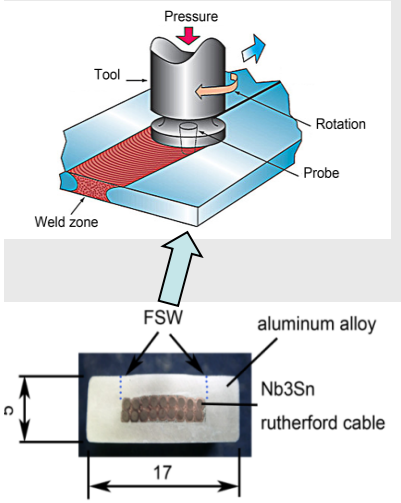

Critical current measurement of the subscale indirect-cooling Nb_3Sn superconductor with aluminum alloy jacket.

Rigidity evaluation of a helical coil for LHD-type fusion reactor

1. The mechanical behaviour of the helical coil was analyzed using a 3-D model and a simplified 2-D axisymmetric model.
2. 2-D axisymmetric model which has the mean radius of curvature can estimate a stress distribution of the helical coil.
3. Using the 2-D model, mechanical behavior of an indirect-cooled superconducting helical coil was evaluated and confirmed that all stress and strain levels for each component was within the permissible value.

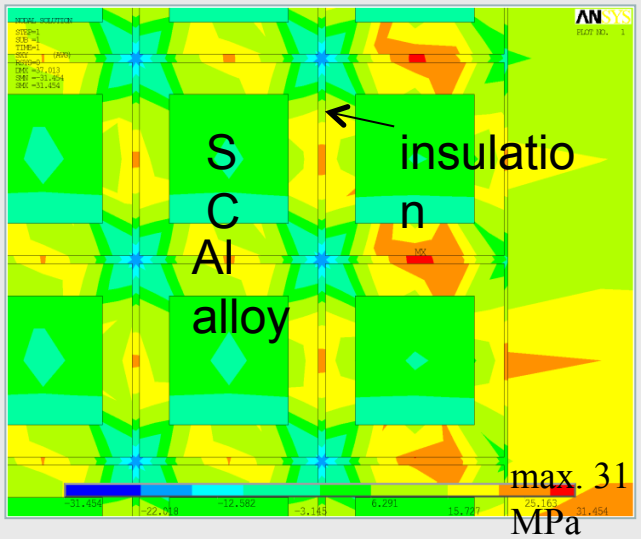

In-plane shear stress distribution in the coil.

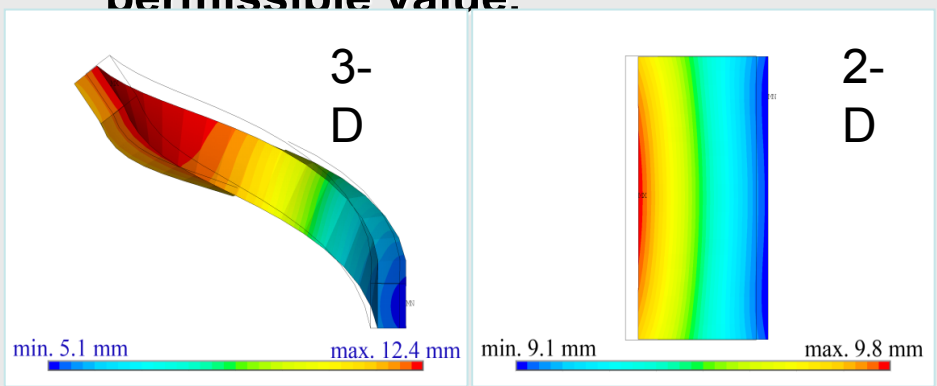

Amount of deformation distribution by the hoop force.

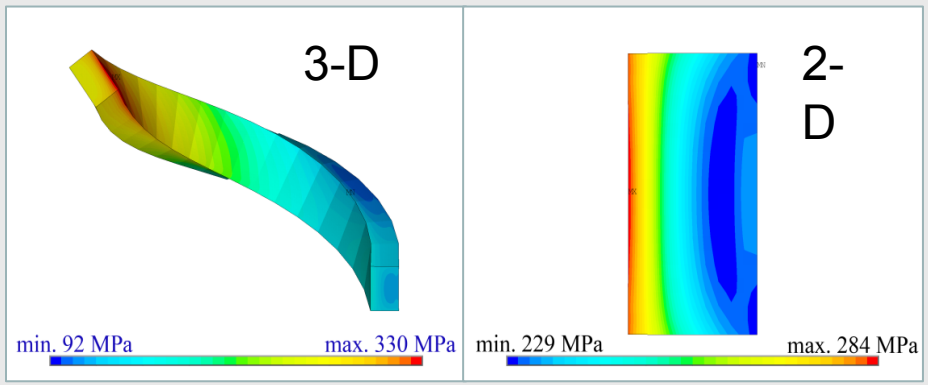

Von Mises stress distribution by the hoop force.

Partition walls in Be pebble layer would largely reduce TBR

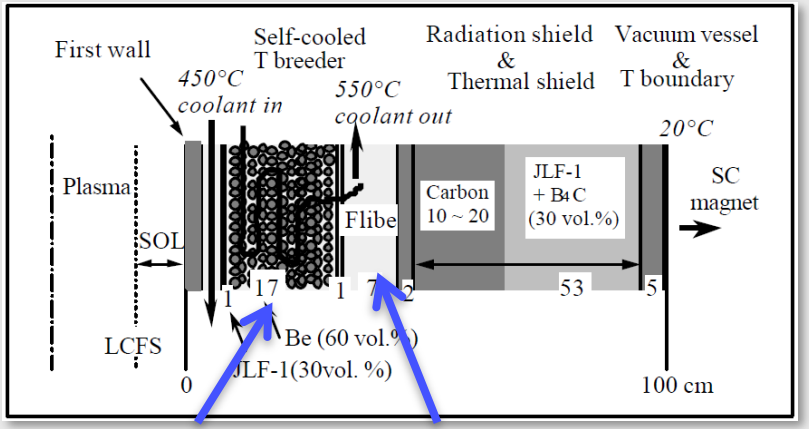

Flibe+Be layer ***2nd Flibe layer***

Structure of Flibe+Be/JLF-1 blanket

<u>Flibe+Be/JLF-1 blanket</u>

Local TBR: 1.26

1st Flibe layer: 14 %
Flibe+Be layer: 69 %
2nd Flibe layer: 17 %

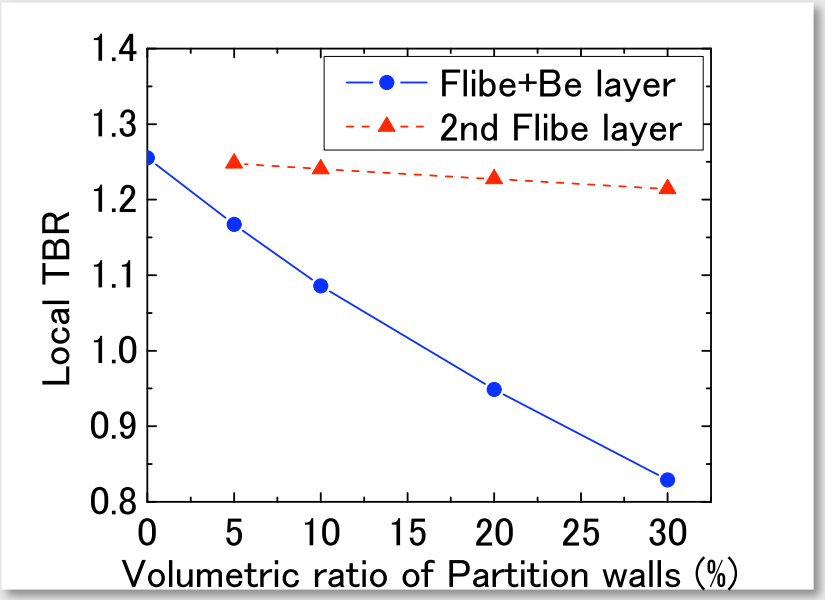

Impact of partition walls on TBR

Tentative calculations (*Flibe, Be and partition walls are uniformly mixed)* showed that insert of partition walls in Be layer would largely reduce TBR.

Detailed blanket structure design from neutronics view point is planned. With enhancement of coordination with thermo-fluid dynamics and structural dynamics researchers.

Tritium recovery apparatus and tritium permeation through heat exchanger for 2-Flibe-loop system for FFHR are calculated and designed.

Kyushu Univ. and NIFS

Presented in SOFT (2008)

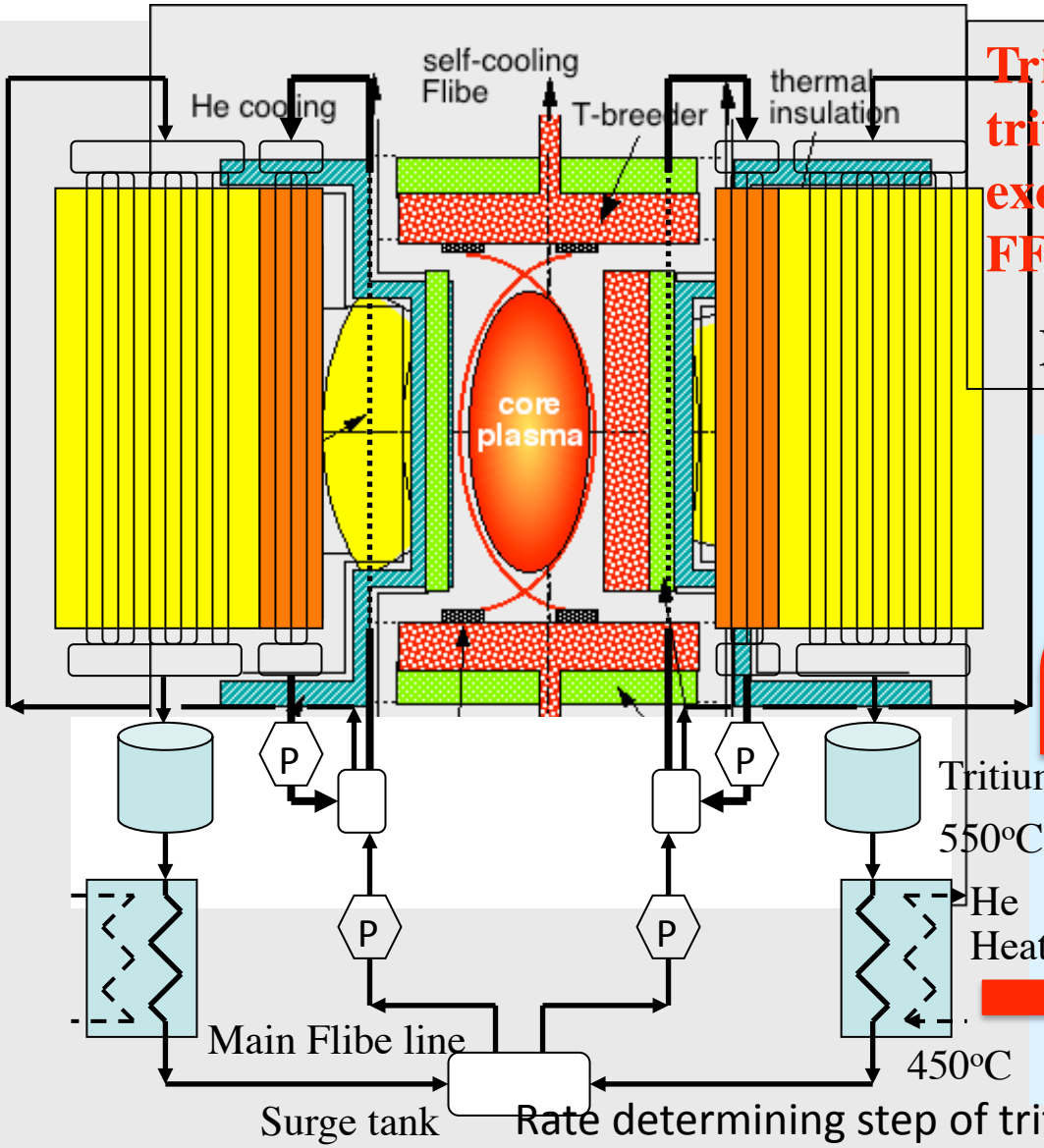

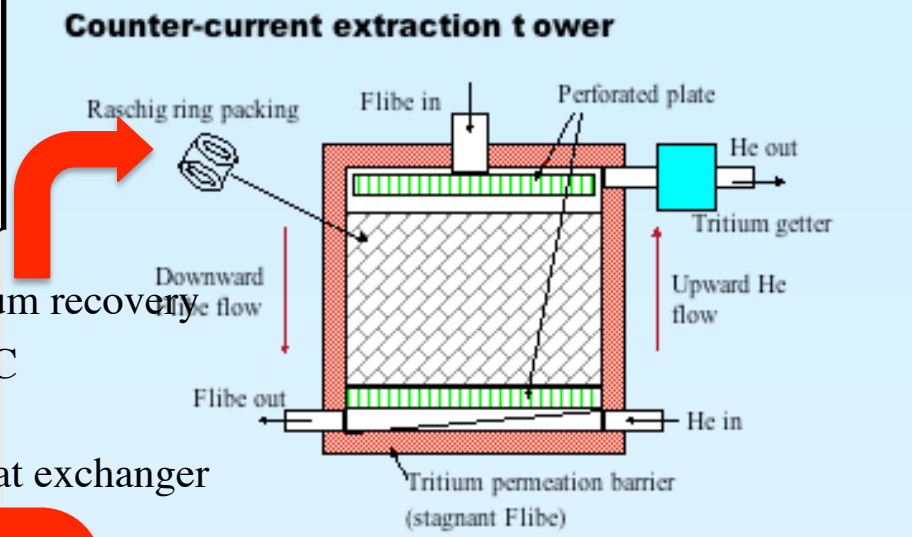

Fig. 8 Flibe-He counter-current ext raction tower

Rate determining step of tritium permeation in Flibe-HX tube system

Breeder	Structural material	Temperature	$S_{wall\text{-}T}D_{wall\text{-}T}$	$S_{breeder\text{-}T}D_{breeder\text{-}T}$	Bi_T
$Li_{17}Pb_{83}$	F82H[8)]	500°C	6.93×10^{-11}mol/msPa$^{0.5}$	9.68×10^{-11}mol/msPa$^{0.5}$	7.2/Sh
$Li_{17}Pb_{83}$	SiC[9)]	800°C	4.06×10^{-8}mol/ms[*2)]	2.60×10^{-10}mol/msPa$^{0.5}$	6.4/Sh
Flibe	V-4Cr-4Ti[10)]	500°C	5.0×10^{-8}mol/msPa$^{0.5}$	4.50×10^{-13}mol/msPa$^{0.5}$	1.1×10^{6}/Sh
Flibe	F82H[8)]	500°C	6.93×10^{-11}mol/msPa$^{0.5}$	4.50×10^{-13}mol/msPa$^{0.5}$	1.1×10^{6}/Sh
			Permeability of wall	Permeability of breeder	Ratio of two permeabilities

Corrosion of RAFM steel JLF-1 (Fe-8.92Cr-2W) can be controlled by impurity control in molten salt

Facilities : Molten-salt compatibility test facilities (NIFS, U-Tokyo)

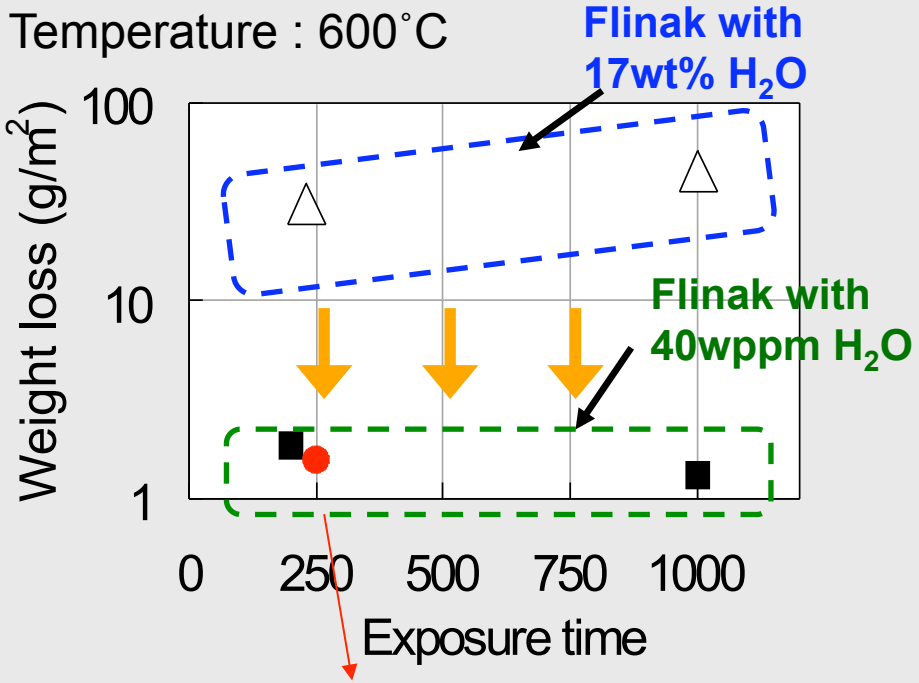

SEM surface Image

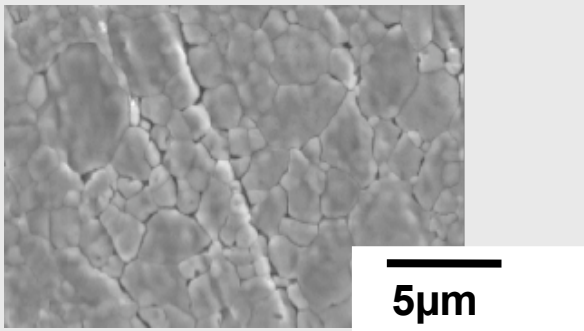

M. Kondo et al., ISFNT-9, Dairen (2009)

1. **Measurement technique** of major impurity of **H_2O** and **HF** in molten salts Flinak and Flibe was established.
2. **Control of Impurity** in molten salt by electro refining was successfully established. Concentration of **H_2O** in molten salt Flinak was drastically decreased by the electro refining.
3. **Corrosion was very small after the electro refining of molten salt Flinak.**
4. **Mass transfer by temperature difference** will be made clear in future work.

Will be presented at IAEA FEC 2010 by M.Kondo

Road map toward steady-state helical DEMO reactor

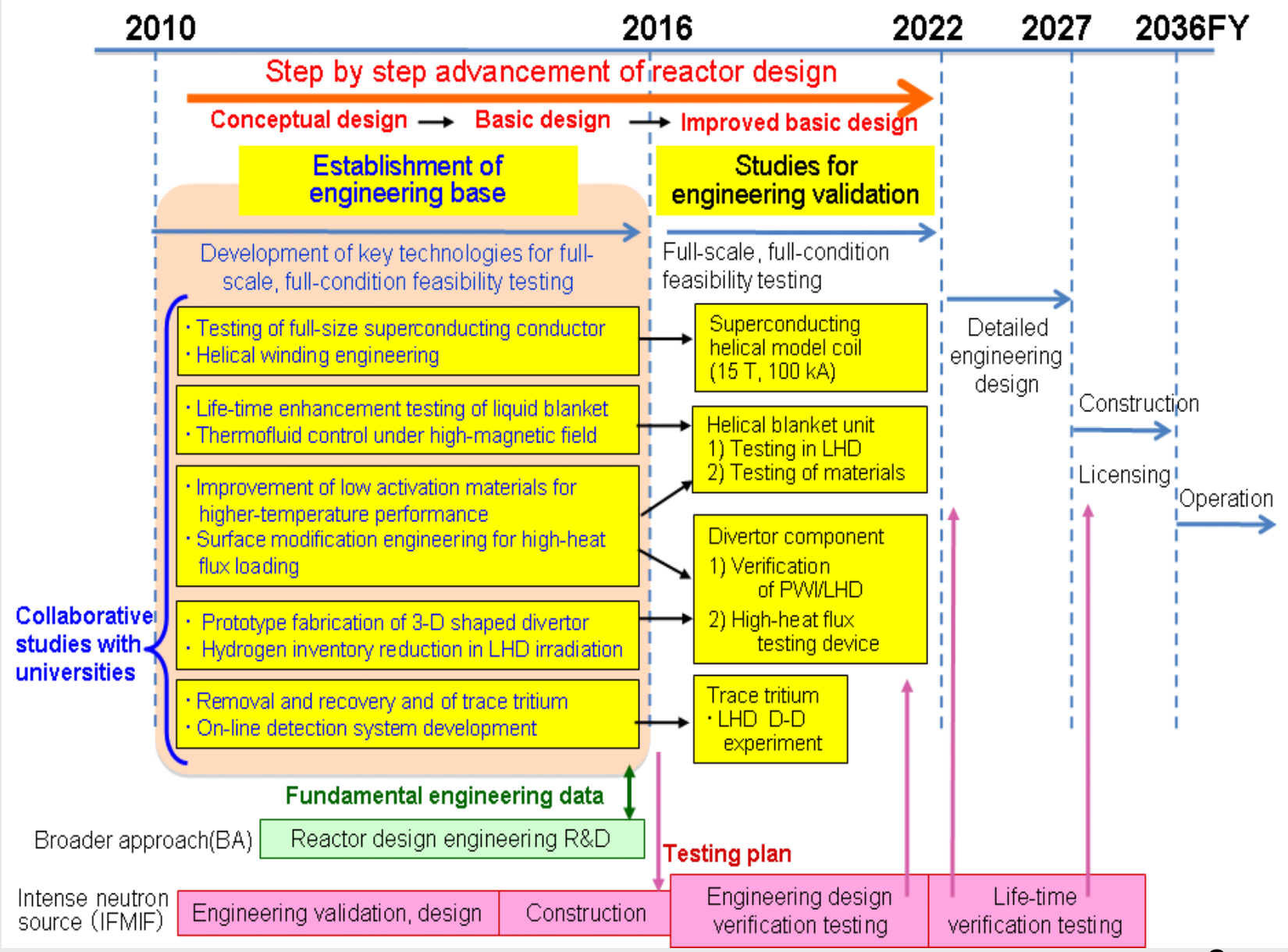

4 projects will start in the new organization for the 2nd Mid-term goal & plan

New Organization (FY2010 ～)

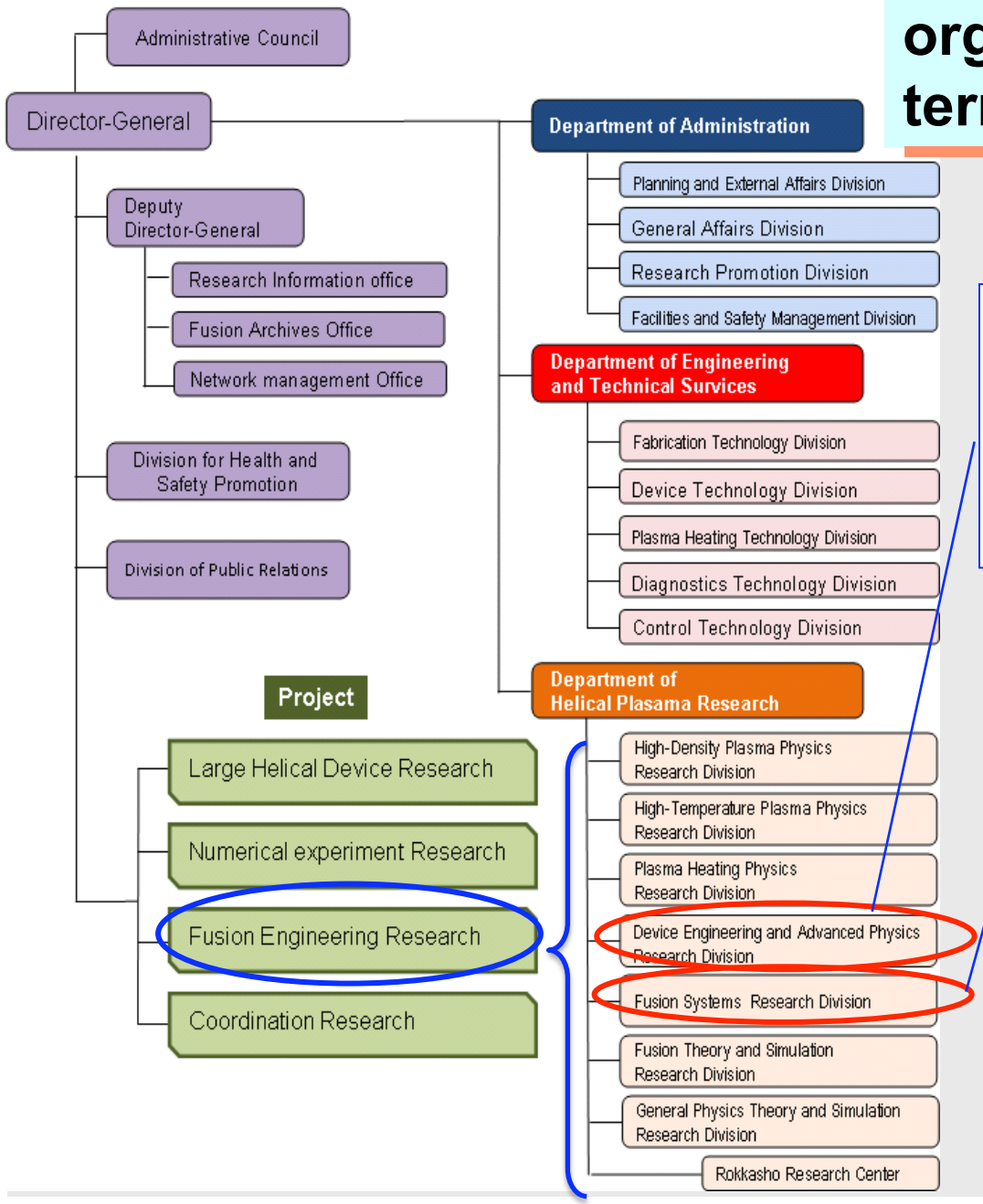

Device Engineering and Advanced Physics Research Division (Staffs: 7,7,4)

- LHD maintenance and D-D safety devices
- Trace tritium monitoring and handling
- Large SC magnet system and applications

Fusion System Research Division (Staffs: 6,5,8)

- Helical reactor DEMO design
- Remote maintenance and replacement
- Low activation materials and long-life liq. blanket
- PWI and high-heat flux components
- Atomic and molecular processes

Concluding remarks

Main advantages are

1. Current-free plasma for steady, CD-free & disruption-free,
   -> High density operation for large reduction of divertor load,
   -> Wide range of start-up time to minimize ex-heating power,
2. Natural divertor.

We are now focusing on key issues of

1. Reactor size optimization for blanket space and mag. energy,
2. Large SC magnet system of 3D or continuous winding,
3. Large maintenance ports and replacement scenarios,
4. R&D's of 3D component mockup studies with design activities.